

# The effect of Coulomb interactions on the ac mobility of charges in quasi-one-dimensional systems. Example: discotic liquid crystals

Laurens D. A. Siebbeles

*Interfaculty Reactor Institute, Delft University of Technology, Mekelweg 15, 2629 JB Delft, The Netherlands*

Bijan Movaghar

*SOMS Centre, Department of Chemistry, University of Leeds, Leeds LS2-9JT, United Kingdom*

(Received 29 March 2000; accepted 24 April 2000)

Using Monte Carlo simulations we calculate the frequency dependence of the diffusive mobility of a group of carriers on a short one-dimensional chain. We allow the carriers to interact with each other through weakly screened long-range Coulomb potentials. We consider both doped systems with discrete immobile counterions and gated systems with constant neutralizing background. In doped systems the counterions can act as traps for the mobile charge, which results in a strong frequency-dependent conductivity. In the gated charged system, the mobility per particle decreases with particle density. The calculations show that the electron–electron interaction, in the diffusion limit, acts very much like a source of random disorder. Because the mobility depends on the number of carriers, arrays of coupled wires can exhibit current “noise” which is directly related to charge exchange between the wires. This noise is in principle observable in signal processing. Basing ourselves on our numerical results, we have been able to conclude that the low-frequency ac mobility measured in doped triphenylenes must be due to spatial charge inhomogeneities, and cannot be due to intrinsic charge dynamics. © 2000 American Institute of Physics.

[S0021-9606(00)70128-0]

## I. INTRODUCTION

Columnar liquid crystals are remarkable examples of systems in which it has been possible to observe quasi-one-dimensional diffusion, drift, and relaxation kinetics up to very high temperatures.<sup>1–10</sup> Quasi-one-dimensional random walks of excitons have been demonstrated by time-resolved fluorescence measurements.<sup>11</sup> Christ *et al.*<sup>12</sup> have shown that it is possible to vapor deposit, spin coat, and then to optimize the electroluminescence yield by aligning columns perpendicular to the substrate. In this way it is possible to achieve double charge injection into molecular columns. The inter-columnar distances of discotics are typically of the order of 2 nm, whereas the intracolumnar disc–disc separation is only about 0.35 nm. The mobility anisotropy can be inferred from the measurements by Warman *et al.*<sup>10,13–15</sup> at high frequencies, and by Boden *et al.*<sup>1,16</sup> at low frequencies, to be of order  $10^3$ . Columnar liquid crystals are self-organizing, the columnar molecular structure continuously breaks and reforms on a time scale of  $10^{-5}$  s.<sup>17</sup> The liquid-like molecular motion along the column and the transverse motion and molecular rotations generate instantaneous disorder which can reduce the long-time carrier diffusivity to values down to  $\sim 10^{-5}$  cm<sup>2</sup>/s. A typical maximum nearest-neighbor hop is of order  $10^{12}$  Hz along the column, whereas the critical hop frequency extracted from the mobility is reduced by disorder to be of the order of  $10^{10}$  Hz.

In this article we continue investigating the role of electron–electron interactions in the transport properties of quasi-one-dimensional systems. The methods developed in this article can be applied to discotic liquid crystals as well as conjugated polymers as long as the stochastic transport

limit is valid. As before,<sup>18</sup> we use discotic liquid crystals as our model system, but there exist other important systems which satisfy the same or similar criteria. Polydiacetylenes (PDAs) are, for example, highly ordered and very anisotropic conjugated polymers. With conjugated polymers, including PDAs, one is usually dealing with materials which appear in bulk form and consist of finite chains with a length which is usually less than 100 nm. Alignment of the polymer chains introduces real and measurable charge transport anisotropy.<sup>19–22</sup> More recently, there have been new brilliant innovations in the fabrication of one-dimensional conducting wires. Using molecular beam epitaxy and nanolithography, some groups have recently succeeded in making quasi-one-dimensional charge doped Ga–As wires which exhibit electronic correlation effects in the transport properties at low temperatures.<sup>23,24</sup> Carbon nanotubes are other brilliant examples of quasi-one-dimensionality in material development. The electrons on nanotubes can also exhibit strong correlations.<sup>25</sup>

In the present work, we are focusing on discotic liquid crystals, but the reader should note that the methodologies we are developing in this article can, and will in the future, be applied to the other new materials mentioned above. We emphasize that present methods can only handle systems in which the transport takes place in the diffusion limit. This implies, in particular, that our theory only applies to conducting “wires” and nanotubes with short electronic mean-free paths. When applying the theory to conjugated polymers we introduce box boundary conditions or tunnelling barriers which simulate chain-end boundary conditions.

The material of this article is organized as follows. In

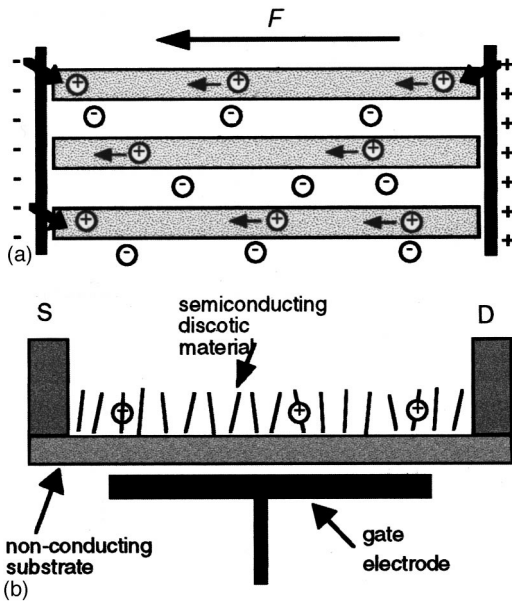


FIG. 1. (a) The doped discotic system. The holes on the column are generated by doping. The counterions are sitting interstitially. The counterions are a source of trapping. The external field is denoted by  $F$ . (b) The gated "jellium" model system. Here the molecular wire is first charged by a gate, then the conduction takes place in the plane between source ( $S$ ) and drain ( $D$ ).

Sec. II we discuss the one-dimensional model systems. In Sec. III we describe the many-body Monte Carlo computer simulation method. In Sec. IV we present results encompassing the mobility of holes moving in the field of counterions [Fig. 1(a)] as well as the mobility of holes in a gated system [Fig. 1(b)]. In Sec. V, we discuss the results and the scope of the future work. In Sec. VI we present a summary.

## II. MODEL SYSTEMS

Our model systems are shown in Fig. 1. The figure shows schematically the one-dimensional columnar wires along which the holes can move. The holes in Fig. 1(a) are produced by chemical doping with, for example,  $\text{AlCl}_3$  or  $\text{NOBF}_4$  in HAT6, (see Refs. 16 and 26. The negative counterions shown in the figure are negative ionic complexes. This doping yields a maximum of up to one charge every 5 nm. Counterions are sitting interstitially, their average location is not known accurately, but they are quite mobile in the liquid crystalline phase.<sup>17</sup> We expect counterions to be on average at a distance of around 1–1.5 nm from the columnar chain. With counterions [Fig. 1(a)], we have charged centers, and the counterions represent serious traps for the charges. The trapping and detrapping constitutes a process which itself gives rise to a strong frequency dependence of the conductivity.

Another interesting limit for the study of correlations is the situation when the charges are produced by a voltage on a gate electrode [see Fig. 1(b)]. In this situation the space charge field is neutralized by the gate field, which does not trap the carriers. The ac response of the gated "jellium" is

expected to be affected by the mutual Coulomb repulsion between the holes.

One can also obtain high carrier concentrations by using single and double injection with high electric fields.<sup>12,27</sup> Here the driving force for charging is the external field, and there is no neutralizing counterion.

### A. The diffusion model applied to a single chain

For spinless carriers (fast relaxing spins with spin lattice relaxation rates much larger than the jump rate), we have on the columnar sites the master equation for the hole density

$$\frac{dH_n(t)}{dt} = -H_n(t)(W_{n,n-1} + W_{n,n+1}) + H_{n+1}(t)W_{n+1,n} + H_{n-1}(t)W_{n-1,n}, \quad (1)$$

which describes the hopping of holes to adjacent sites, with  $H_n(t)$  denoting the hole density at site  $n$  at time  $t$ . The transition rates in an oscillating external electric field  $F(t) = F_0 \cos(\omega t)$  are given by

$$W_{n,n\pm 1} = \begin{cases} \nu_0 \exp\left[-\frac{V_{n\pm 1} - V_n \mp eFa}{kT}\right] & \text{for } V_{n\pm 1} - V_n \mp eFa > 0, \\ \nu_0 & \text{for } V_{n\pm 1} - V_n \mp eFa \leq 0. \end{cases} \quad (2a)$$

These expressions are valid for time-dependent fields as long as one works in the limit where the transition takes place on a time scale, which is faster than the inverse frequency of the field. In the present work, we are dealing with rates which are of order  $10^9$  to  $10^{12}$  Hz, so frequencies of up to, say,  $10^{10}$  Hz are reasonably well described with this approach. For frequencies higher than this value, one cannot argue that the field simply changes the energy of the final state. Its effect on the transition becomes more complex. This is especially true for frequencies which become comparable to phonon frequencies. In this article we shall nevertheless ignore these problems and stay in the simple semiclassical picture. At very high frequencies, our method will be sampling the very fast "hopping transitions." The slower ones do not follow the field. This is true in the classical as well as in the quantum limit. Only the classical energy shift effect is included in this treatment.

For the model system shown in Fig. 1(a), in which counterions are present at fixed interstitial positions between the conductive columns, the total Coulomb energy of a hole at position  $x_n$  on the column is given by the sum of the repulsion due to the other holes,  $V_{n,\text{rep}}$ , and the attraction by the counterions,  $V_{n,\text{att}}$ , i.e.,

$$V_n = V_{n,\text{rep}} + V_{n,\text{att}} = \frac{e^2}{4\pi\epsilon_0\epsilon_r} \left[ \sum_m \frac{H_m(t)}{|x_n - x_m|} - \sum_i \frac{Q_i}{\sqrt{(x_n - x_i)^2 + d^2}} \right]. \quad (3)$$

The distance of a counterion in the side chain region from the column is given by  $d$  and  $Q_i$  is the occupation number of

a counterion adjacent to site  $i$ .

In the model system of Fig. 1(b) the counterions are due to the negative voltage on the gate electrode starting at a distance  $L_G$  from the electrodes. In this case the jellium or

mean field treatment is applicable to describe the Coulomb energy due to the negative charges on the gate electrode. For  $N_{\text{neg}}$  negative charges and a column with length  $L$  the Coulomb attraction energy for a hole at position  $x_n$  is given by

$$V_{n,\text{att}} = \begin{cases} \frac{e^2}{4\pi\epsilon_0\epsilon_r} \frac{N_{\text{neg}}}{L-2L_G} \ln \left( \frac{L-L_G-x_n + \sqrt{(L-L_G-x_n)^2 + d^2}}{L_G-x_n + \sqrt{(L_G-x_n)^2 + d^2}} \right), & x_n < L_G, \\ \frac{e^2}{4\pi\epsilon_0\epsilon_r} \frac{N_{\text{neg}}}{L-2L_G} \ln \left( \frac{(x_n-L_G + \sqrt{(L_G-x_n)^2 + d^2})(L-L_G-x_n + \sqrt{(L-L_G-x_n)^2 + d^2})}{d^2} \right), & L_G \leq x_n \leq L-L_G, \\ \frac{e^2}{4\pi\epsilon_0\epsilon_r} \frac{N_{\text{neg}}}{L-2L_G} \ln \left( \frac{x_n-L_G + \sqrt{(x_n-L_G)^2 + d^2}}{x_n-L+L_G + \sqrt{(x_n-L+L_G)^2 + d^2}} \right), & x_n > L-L_G. \end{cases} \quad (4)$$

The many-body energy difference for a jump on the conductive column from  $x_n$  to a neighboring site  $x_{n\pm 1} = x_n \pm a$  is simply

$$K_{n,n\pm 1} = V_{n,n\pm 1} - V_n \mp eFa, \quad (5a)$$

with  $a$  the distance between adjacent columnar sites.

Carriers can also enter and leave the columns from the electrodes. When the Fermi level of the metal electrode has an energy  $E_b$  above the valence band of the organic material the energy difference for hole injection from the electrode to the first site ( $n = 1$ ) is

$$K_{n=1}^{\text{inj}} = E_b + V_{n=1} - eFa, \quad (5b)$$

and for injection to the last site ( $n = N$ ) the energy difference is

$$K_{n=N}^{\text{inj}} = E_b + V_{n=N} + eFa. \quad (5c)$$

The energy differences for a hole leaving the column from the first site is

$$K_{n=1}^{\text{abs}} = -E_b - V_{n=1} + eFa, \quad (5d)$$

while for leaving the column from the last site the energy difference is

$$K_{n=N}^{\text{abs}} = -E_b - V_{n=N} - eFa. \quad (5e)$$

In addition we also consider systems in which the electrodes act as fully reflecting boundaries and neither charge injection nor absorption occurs at the electrodes. These box-like boundary conditions correspond to  $K^{\text{inj}} = K^{\text{abs}} = \infty$ .

To get an insight into the value and possible consequences of many-particle transport physics, it is worth first considering the novel science that a stochastic transport picture cannot take into account. Let us examine what processes the present approximation cannot see, and how worthwhile an improved treatment in the future might be.

### B. The classical limit: Coherence and force

Consider what would happen if we treated the same system of holes shown in Fig. 1(a), for example, using classical dynamics. The Drude equations for each charge now becomes

$$m d^2 x_i / dt^2 + \gamma dx_i / dt = -\nabla_i V(x_i) + eF_0 \cos(\omega t). \quad (6)$$

The many-particle potential is given by Eq. (3). Looking at the many-body force term, one immediately sees that one is dealing with a coupled system of nonlinear equations which can only be solved numerically. The current is given by

$$I = e \sum_i dx_i(t) / dt \quad (7)$$

and will exhibit complex nonlinear dynamics. Some of this new complexity can be extracted if we look at the force in the harmonic limit and put  $x_i(t) = n_i a + \delta x_i(t)$ , where the displacement is relative to an equilibrium point along the coupled string. Then it follows that one can think of the particles as being attached to strings similar in a way to atoms by nearest-neighbor forces as in the treatment of lattice dynamics. This is essentially the Frenkel-Kontorova model (see Ref. 28). This is also the classical limit of the quantum ‘‘Luttinger liquid.’’ This problem is very topical (see, for example, Refs. 23 and 24). In the limit that random forces dephase the deterministic Coulomb forces, one can work in the stochastic picture. Up to now we have assumed that we have a one-dimensional wire. Now let us examine some consequences of three-dimensionality.

### C. The role of three-dimensional charge fluctuations

In this section we examine how important it is to look at the coupling between the wires. We shall show that however weak the coupling, there is some qualitatively new and important science.

Carriers can jump from chain to chain (with a typical frequency of  $10^5$  Hz), thus causing charge and particle fluctuations. This allows us to describe the system as a three-dimensional ensemble of coupled wires. Since the charging

step from two neutral columns  $\{N, N\}$  to a negatively and a positively charged column  $\{N-1, N+1\}$  is normally energetically unfavorable, the neutralizing return step has a higher rate, and such configurations can then be considered to be excited states of the neutral system of columns. If we call  $\sigma(N+m)$  the conductivity of a single column charged with  $N+m$  charges and  $N$  counterions, then since the columns conduct in parallel, we can write down an expression for the thermal average quasi-three-dimensional conductivity assuming that we know the distribution function  $P$  for charged chains. The latter depends simply on the energy of the charged chains

$$\langle \sigma(\omega) \rangle = \sum_m P(E_{N+m}) \sigma(N+m, \omega), \quad (8)$$

where  $P_{N+m}$  is the probability that a chain or column has  $N+m$  charge carriers and  $N$  counterion particles.

In the discotic liquid crystals, only single charge fluctuations are likely to occur from column to column, and they will not dramatically change the value of  $\sigma(N)$ . Consider for illustration two coupled chains so that the total current through the pair is

$$I(t) = (eN_1(t)\mu(N_1) + eN_2(t)\mu(N_2))F(t), \quad (9)$$

with  $\mu(N)$  the mobility per carrier on a column with  $N$  carriers. When the total number of charges  $N_c$  is conserved,

$$N_c = N_1(t) + N_2(t), \quad (10)$$

$$N_1 = N_0 + b(t), \quad N_2 = N_0 - b(t). \quad (11)$$

To first order the current fluctuation is

$$\delta I(t) \sim 2eN_0b(t)(\delta\mu/\delta N). \quad (12)$$

If the mobility is constant and independent of the charge concentration on each chain, the effect of charge exchange is zero. If, on the other hand, the interactions cause the mobility on a chain to depend on the number of charges as they normally would in interacting systems with traps, then, by looking at the current noise both in real time and in Fourier space, one can monitor the dependence of the mobility on the number of charges  $N$ . To model a real experiment one would have to distinguish between random noise generated by trapping and detrapping from the noise which is a result of the many-body effects. This can be done by also looking at the doping dependence of the ac noise. The smaller the electrode size and the thinner the cell, the more pronounced such cross-talk noise will be.

Three dimensionality, however weak the coupling between wires may be, gives rise to yet another important effect. This has to do with the electric field produced by the electrodes. Charge injected into a single column generates an image charge in the electrode from which it is coming, and this image is fairly localized around the molecule, which is attached to the interface. In a purely one-dimensional column, the field due to the image charges would be Coulomb-like. The field is also very efficiently screened inside by intermediate charges resident on the same column. This is, of course, very different when we consider a real three-dimensional array of columns. Here the action of many col-

umns gives rise to a uniform constant field deep in the bulk, and the screening is also qualitatively different. It is, however, also worthwhile to think in terms of making truly single columns or thinly spread arrays of columns. Columnar separations of 5 nm are already realizable now with long chain mesogens. Such ‘‘isolated’’ columnar arrays will have very different internal fields close to interfaces.

### III. MONTE CARLO SIMULATION PROCEDURE

The computer simulation procedure is similar to that used in the work of Ref. 18. The present simulations differ by the fact that the time dependence of the oscillating external electric field needs to be taken into account.

The mobility of the holes is related to their time-dependent positions  $x_j(t)$  according to

$$\mu_j = \frac{1}{F(t)} \frac{dx_j}{dt}. \quad (13)$$

In the simulations jumps occurring at times for which  $F(t) = F_0 \cos(\omega t) \sim 0$  create a large numerical noise if the mobility is calculated by use of Eq. (13). In analogy to the work of Refs. 29 and 30 we therefore obtain the mobility from the work done by the electric field on the charges. The performed work during a time interval  $dt$  is

$$dA = e \sum_j F(t) dx_j(t), \quad (14)$$

where the summation runs over all holes in the system. Substitution of Eq. (13) into Eq. (14) and integration over an oscillation period of the external field, i.e.,  $\Delta t = 2\pi/\omega$ , gives for the average hole mobility

$$\mu = \frac{2\Delta A}{eF_0^2\Delta t N_h}, \quad (15)$$

with  $\Delta A$  the total work done on all the holes during  $\Delta t$  and  $N_h$  the number of holes in the system.

In the computer simulations of hole transport in the doped system of Fig. 1(a) the positions of the immobile counterions along the columnar direction were taken such that they are at least 1.4 nm away from the electrodes. The energy due to the Coulomb repulsion between the counterions has a minimum value if these are positioned at equal distances along the columnar direction. In the simulations we have uniformly distributed the counterions along the columnar direction in such a way that the change of the Coulomb repulsion energy due to displacement of a counterion from the equilibrium configuration does not increase the Coulomb repulsion by more than  $k_B T$ . Note that the positions of the counterions along a column are fixed in time. The counterion positions only differ from one column to another. The Coulomb energy of the holes in the doped system is given by Eq. (3). In the jellium model system of Fig. 1(b), the attractive Coulomb energy was calculated from Eq. (4) with the distance  $L_G$  taken equal to 1.4 nm.

For the doped system of Fig. 1(a), the holes are initially, i.e., at time  $t=0$ , placed at the same position along the columnar direction as the negatively charged counterions. These initial positions were also used for the holes in the

gated system of Fig. 1(b). For all holes on the column, the frequency for a jump to a neighboring site on the column was calculated using Eqs. (3), (4), and (5a) with  $\nu_0 = 10^{12}$  Hz,  $\epsilon = 3$ ,  $T = 293$  K, and  $a = 0.35$  nm. The amplitude of the electric field was taken to be  $F_0 = 2 \times 10^6$  V/m. The frequency for hole injection or absorption by the electrodes was calculated using the energy differences in Eqs. (5b)–(5e). The holes were not allowed to jump to a site on the column which is already populated by another hole. For each hole the time,  $\delta t$ , after which it jumps was sampled from the exponential distribution  $\exp(-(W_{n,n-1} + W_{n,n+1})\delta t)$  by using the expression  $\delta t = -\ln(R)/(W_{n,n-1} + W_{n,n+1})$ , with  $R$  a uniformly distributed random number in the interval  $\langle 0,1 \rangle$  (see Ref. 31). The hole for which the shortest time after which it jumps,  $\delta t_{\min}$ , has been sampled is allowed to perform a jump, provided  $\delta t_{\min}$  is sufficiently small such that the electric field can be considered constant during  $\delta t_{\min}$ . It was found that for  $\delta t_{\min} < 2\pi/50\omega$  the change of the electric field during  $\delta t_{\min}$  could be neglected.

When a hole on the column jumps to a neighboring site the probability to jump from the site  $n$  to the site  $n \pm 1$  is equal to  $P_{n,n \pm 1} = W_{n,n \pm 1} / (W_{n,n+1} + W_{n,n-1})$ . A random number  $R'$  in the interval  $[0,1]$  is used to decide whether the hole jumps to the site  $n-1$  or the site  $n+1$ . If  $R' < P_{n,n-1}$ , the hole jumps to the site  $n-1$ ; otherwise it jumps to the site  $n+1$ . After the jump has occurred the time is increased to  $t + \delta t_{\min}$ . When a hole makes a jump to from site  $n$  to the site  $n \pm 1$  the work done by the external electric field is calculated according to  $\pm eaF(t)$  and added to the total work done at the time of the jump,  $\Delta A(t + \delta t_{\min})$ , from which the mobility can be calculated using Eq. (15). Then the Coulomb energy with the new position of the hole that has jumped is calculated and the above procedure is repeated for the next jump until a final preset value of the time has been reached.

If the sampled minimum jump time  $\delta t_{\min} > 2\pi/50\omega$ , the jump is not allowed to occur. In that case the time is increased to  $t + 2\pi/50\omega$ , the field strength at this time is calculated, new jump rates are determined for all holes, and the above procedure is repeated until the preset final time has been reached.

Due to hole injection and absorption at the electrodes the number of holes on the column initially varies in time and reaches a steady value which is determined by the value of  $E_b$  in Eq. (5). A positive value of  $E_b$  corresponds to a barrier for hole injection, which reduces the injection rate with respect to the hole absorption rate by the electrodes. In that case the number of holes will initially decrease with time. When the number of holes on the column decreases the repulsive Coulomb energy between the holes becomes smaller, which enhances the injection rate and reduces the absorption rate [via the repulsive term in  $V_{n=1,N}$  in Eqs. (3) and (5)] until a steady value of the number of holes on the column has been reached. The simulations were proceeded to times for which the number of holes had reached a steady value. The value of  $E_b$  was chosen such that the steady number of holes on the chain was close to the number of negative ions. The average mobility of the holes was calculated from

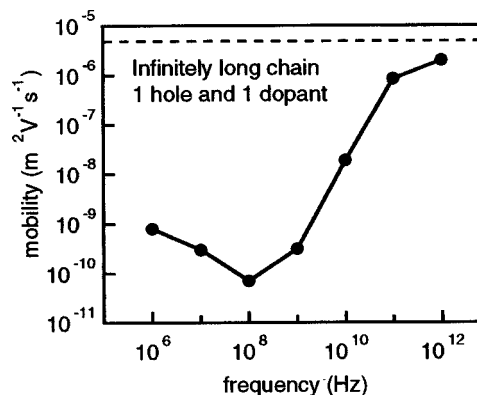


FIG. 2. The mobility for one hole on an infinitely long column moving in the Coulomb field of one discrete negative ion (dopant), which is positioned at a distance 1 nm from the column. For comparison the mobility of a free hole on an infinitely long chain is given by the dashed line.

$\Delta A(t)$  at times for which the number of holes had reached a steady value, using Eq. (15).

To obtain the average mobility for many columns the simulations were carried out with different series of random numbers. The use of different series of random numbers results in a different stochastic motion of the holes and, in the case of the model system of Fig. 1(a), it results in columns with different positions of the counterions.

#### IV. RESULTS OF THE EXACT MANY-PARTICLE SIMULATIONS

We have considered the two distinct systems depicted in Figs. 1(a) and 1(b), corresponding to a doped system with discrete negative counterions and a system with a gate electrode, respectively.

##### A. Doped system

Figure 2 illustrates the situation when we have one hole and one negatively charged counterion on an infinitely long chain. The counterion is placed at a distance  $d = 1$  nm from the chain. The hole is allowed to diffuse in the presence of the external oscillating field and the counterion field. At low frequency, the hole has a low mobility because it has to escape up the Coulomb potential hill in order to follow the external electric field. In the long time limit it can escape to infinity. The zero frequency value should therefore eventually saturate at the free carrier value. The data shows that at  $10^6$  Hz, we are still very far from this limit. Note that the distance,  $R_c$ , that the hole needs to travel before it can escape to infinity in a constant electric field  $F$  is given by the maximum in the potential which is given by  $F = e/(4\pi\epsilon_0\epsilon(R_c + d)^2)$ . For  $F = 2 \times 10^6$  V/m,  $d = 1$  nm,  $\epsilon = 3$  we find that  $R_c \sim 10$  nm. For a field frequency of 1 MHz, the mobility in Fig. 2 is about  $10^{-9} \text{ m}^2 \text{ V}^{-1} \text{ s}^{-1}$  and the distance the hole travels during an oscillation period of the field is about 1 nm, which is much less than  $R_c$ . Hence at 1 MHz, the hole does not yet escape from its counterion. At high frequencies, the hole can oscillate backwards and forwards near the counterion. The high-frequency saturation value is determined by the rate to jump from the origin to the next neighbor. This constitutes the worst single jump rate and is

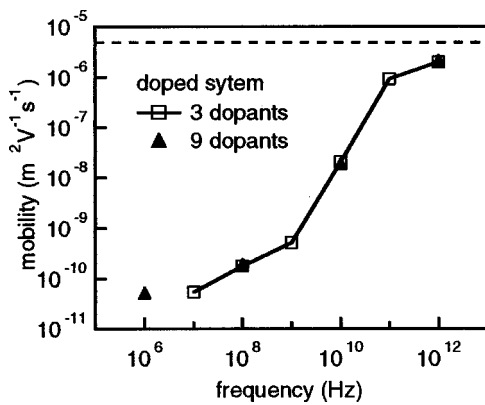


FIG. 3. The mobility per hole as a function of frequency for the case of three and nine discrete negative ions (dopants) adjacent to the column at a distance  $d=1$  nm. For comparison the mobility of a free hole on an infinitely long chain is given by the dashed line.

given by  $\nu_0 \exp(-E_A/kT)$  with the activation energy  $E_A = e^2/(4\pi\epsilon\epsilon_0)(1/d - 1/(d^2 + a^2)^{1/2})$ . For  $d=1$  nm and  $a=0.35$  nm, we have a maximum rate  $W_{\text{hole}} \sim 10^{11}$  Hz. These two extrema, together with the fact that the high-frequency motion is symmetric about the origin, and the fact that the low-frequency motion is not symmetric explain the minimum in the data in Fig. 2 (the carriers in this limit are either to the left or to the right of the counterion during the period of the field).

Figure 3 shows the mobility per hole on a chain of 300 sites between two electrodes for three or nine counterions adjacent to the chain, [see the model system of Fig. 1(a)]. The charge injection and absorption rates at the electrodes are determined by the activation energies in Eq. (5). The value of  $E_b$  (the Fermi level difference before the system equilibrates) was taken to be 0.5 eV, for which the actual number of holes on the chain is close to the number of counterions (see Fig. 4). Figure 3 shows that the mobility is strongly frequency dependent. At low frequencies the mobility is much smaller than that of a free hole since, in order to follow the external electric field, the holes need to overcome the attractive Coulomb potential due to their counterion. At high frequencies, each hole moves in a limited spatial interval within the Coulomb wells due to its counterion, so the

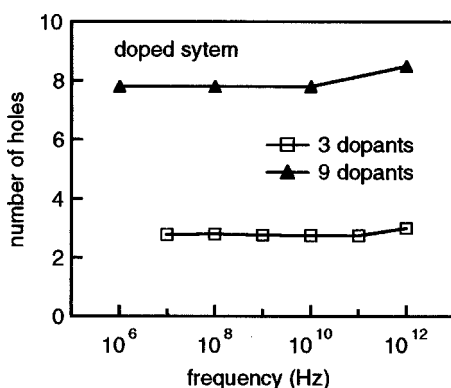


FIG. 4. The number of holes as a function of frequency for three and nine negative ions (dopants) adjacent to the column at a distance  $d=1$  nm. Neutrality is reached at very high frequencies.

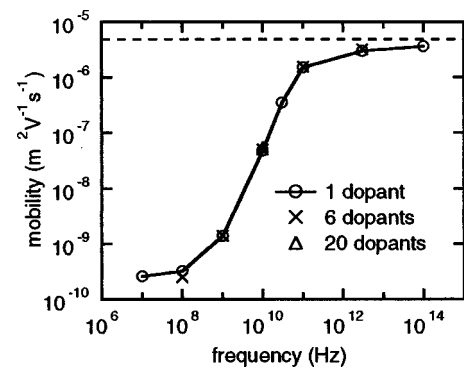


FIG. 5. Mobility per hole for a closed system of 500 sites, with counterions at  $d=1.2$  nm from the column for different counterion concentrations. Note there is no dependence on concentration.

mobility will eventually reach the value for a single hole in the high-frequency limit. The data in Fig. 3 also shows that the mobility per hole does not depend on the concentration of counterions, which is due to the fact that each hole moves predominantly within the Coulomb well due to its counterion. The latter is confirmed by the data in Fig. 5 for a system with discrete counterions and totally blocking electrodes. The ac mobility per hole does not depend on concentration, which demonstrates that each hole moves near its own counterion. This result may seem to be somewhat disappointing, but it also perhaps explains why one-particle physics works so well, at least in this frequency range. However, as we have shown in a previous study,<sup>18</sup> the dc mobility decreases with the counterion concentration, since in a dc field the holes need to move from one Coulomb well to the next. The hindrance of the motion of holes by the Coulomb wells becomes more significant as the counterion concentration increases, which leads to a smaller hole mobility.

## B. Gated system

Next we consider the system in which the counterions are treated as a negative background which ‘insures’ charge neutrality [see Fig. 1(b)]. This simulates the situation where the charge has been injected by a metal gate, which starts at a distance  $L_G$  and ends at the same distance from the other electrode. The negative charges on the gate do not act as traps and therefore do not cause on their own any frequency dependence of the mobility. Any frequency dependence in the response must be entirely due to either the effect of the interaction with the contact, or due to the hole–hole interaction.

Figure 6 shows the simulated ac response of holes on a column of 300 sites for different densities of negative charges uniformly distributed at a distance  $d=1$  nm from the column starting at a distance  $L_G=1.4$  nm from the electrodes. The value of  $E_b$  was taken equal to 0.18 eV for which the number of holes on the chain was found to be close to the number of negative counterions on the gate. The mobility per hole depends on frequency. Figure 7 shows that the number of holes on the column is close to the number of negative charges. The variation with frequency is actually much smaller than in the system of Fig. 1(a) with discrete counter-

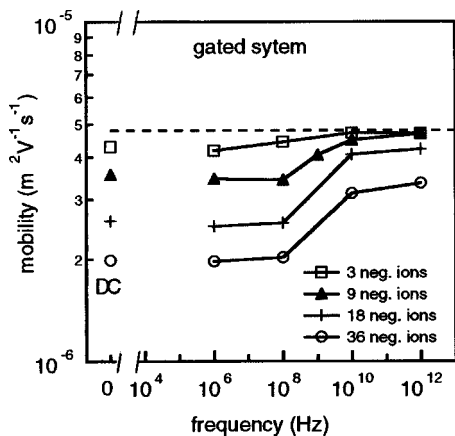


FIG. 6. The mobility per hole for the gated “jellium” model system with different numbers of uniformly distributed negative charges adjacent to the column. The dashed line is the mobility of a free charge on an infinitely long chain.

ions. Figure 6 shows that the magnitude of the mobility per hole decreases with the concentration of holes, and the frequency dependence becomes more pronounced. In fact, the calculation suggests that the metal/organic/metal system behaves exactly as if the mutual interactions between the holes are producing disorder (see also the results of Fig. 8). This result is very interesting in its own right and perhaps not totally unexpected. In a stochastic phase incoherent transport situation, the holes get into each other’s way, and they do that in a random fashion. Deviations from this rule can occur if many holes happen to move in the same direction. The fact that the mobility depends on concentration should now be viewed in conjunction with the predictions made using Eq. (12). Here we predicted that one may be able to observe an ac conductivity and a “cross talk noise” which is a result of Coulomb interactions.

In contrast, the closed system in the jellium model behaves quite different from the closed system with discrete counterions, cf. Figs. 5 and 8. In Fig. 8 one observes that there is, in the case of the jellium model, a relatively strong

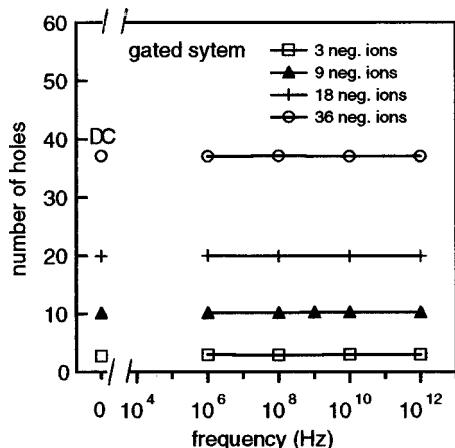


FIG. 7. The number of holes along the column for the gated system with different numbers of negative charges uniformly distributed adjacent to the column. Note that there is a slight charging effect but almost no change with frequency.

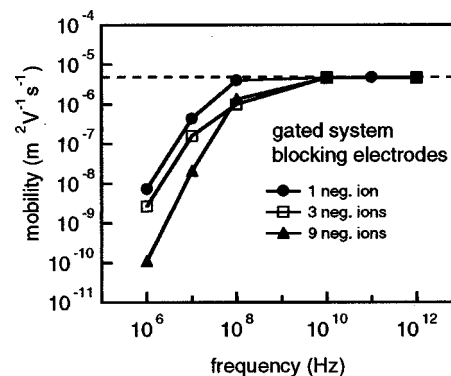


FIG. 8. The gated system with blocking electrode contacts. In the region below 100 MHz the carriers are affected by the boundary and interactions become pronounced. The dashed line corresponds to the mobility of a free hole on an infinitely long chain.

concentration dependence as soon as the holes are beginning to see the confinement produced by the closed system. The mobility decreases with particle number and this is intuitively clear, but it does so at a different rate for different concentrations. For high concentrations, the mobility is lower. This shows that holes are getting “into each other’s way” as they approach a chain end, which is more important at low frequencies. The holes nearest to the boundary are those which are the most strongly confined by their nearest-neighbor charge.

## V. DISCUSSION

Experimentalists have now demonstrated that quasi-one-dimensional “conductors” including molecular wires, semi-conducting wires, and quasi-one-dimensional nanotubes<sup>25</sup> can actually be fabricated in the laboratory using nanolithography self-assembly, combined with evaporation and Langmuir–Blodgett (LB) methods.<sup>32</sup> The situation depicted in Fig. 1 is relatively “easily” realized in the laboratory, at least for finite columns of length  $\sim 100$  nm. Molecular wires based on discotic liquid crystals are at present restricted to operate in the liquid crystalline phase. This implies relatively high temperatures (40 to 150 °C). The finite doped column is realizable experimentally in a number of ways, including making lyotropic discotic liquid crystals and LB films. In all these cases, the carrier motion has a short mean-free path and is well in the domain of stochastic transport. This is exactly the domain of validity of the present theory as well and we can therefore, in principle, use such materials to study Coulomb correlation effects. The point to note is that workers in this field have, until now, not explicitly looked for charge correlation effects because they did not know what to expect and where to look for changes. We hope that this article, which still represents only a modest and initial contribution to the problem, can motivate more experiments on these exciting new materials.

In our previous article<sup>18</sup> we showed, using simulation, that carrier interactions can explain current oscillations which in real time look like noise, but are actually a result of nonlinear deterministic Coulomb interactions between charges. Coherent effects which look like noise are impor-

tant. They may, in fact, be signals which can be associated with the dynamics of “interacting self-organizing charges.” These coherent signals can be hidden in complicated time-varying current signals. In some cases they are due to coherent many-body responses. The way to extract these signals is to look at the current in frequency Fourier space, average out the noise, and pick up remaining well-defined resonances.<sup>33</sup> Generating, understanding and manipulating this type of interaction dynamics can perhaps lead to a new generation of ultra-sensitive chemical and optical sensors (see Ref. 33). According to our previous article<sup>18</sup> the coherent signals observed in Ref. 33 can be identified as being due to periodic creation and destruction of space charge barriers which are created near real barriers (obstacles). This is the way time-dependent self-oscillating signals can be generated in situations when the motion is purely diffusive. In this limit, force or quantum coherent do not influence the dynamics. The carriers see “forces” only in as much as they produce energy differences. In the present paper we have argued that when force and acceleration come into play, it is also possible to expect (coherent) resonances in the ac response. The new modes may be low enough in frequency so that they can be detected outside the usual optical range ( $10^8$  to  $10^{14}$  Hz) and inside the usual impedance analyzer range ( $10^3$  to  $10^8$  Hz).

One of the central aims of this work was to explain the experimental frequency-dependent conductivity data in doped molecular wires.<sup>16,26</sup> The appropriate model is therefore the data shown in Fig. 3. Using our simulation results, we can conclude that the reason for the experimentally observed low-frequency dependence cannot be due to electron–electron interactions or to trapping or to disorder. It is known from hopping theory<sup>28</sup> that in a homogeneously disordered system, the onset of the frequency dependence of ac mobility gives a direct measure of the critical hopping rate which determines the dc mobility of the system. We could, by introducing sufficiently strong disorder and slow enough hopping rates, in principle generate a critical (rate determining) hopping frequency which matches exactly the measured onset. If we try to reproduce the “low onset” of the frequency dependence of the mobility reported in Refs. 16 and 26 ( $\sim 10^5$  Hz) we obtain an absurdly low value of the long time mobility which is  $\mu \sim 10^{-12} \text{ m}^2 \text{ V}^{-1} \text{ s}^{-1}$  (or  $D \sim 10^{-14} \text{ m}^2/\text{s}$ ). Calculations suggest that the observed frequency dependence in Refs. 16 and 26 can only be explained when one allows interfacial barriers to the electrodes in addition to space charge barriers due to Fermi level realignment. In order to understand the data, it is therefore necessary to include the inhomogeneity caused by the interface and the slower injection rates. The low-frequency ac onsets observed in almost all such materials is connected to the fact that carriers have to be injected and extracted from the sample via electrodes which are almost never ohmic. What we see at low frequencies in such thin cells is the impedances at the interface caused by ionic motion and charge injection. The characteristic frequencies in Refs. 16 and 26, for example, are in the range  $10^4$  to  $10^6$  Hz, much lower than anything we see in our calculations when we neglect interface barriers. The particle–particle-induced frequency dependence predicted in this work does not explain the effect; the predictions still

have to be verified by suitably designed experiments. The simulation will have to include an interfacial barrier, while experiments should ideally also be done at higher frequencies than  $10^6$  Hz.

## VI. SUMMARY

We have shown that Coulomb forces acting between weakly screened charges in thin cells have new and interesting and perhaps technically useful consequences. We have argued that Coulomb interactions can give rise to new ac absorption modes, which can have very low frequencies. These could, in principle, be seen in voltage pulsed Fourier transform experiments. According to our computer simulations the frequency dependence of the charge carrier mobility is larger in a doped system than in a “jellium” system in which charges are created by a gate voltage.

In the doped system the mobility of a charge carrier approaches that of a free carrier only when the field frequency is close to the attempt frequency for jumping of the charge carrier. In the doped system the mobility was found not to depend on the charge density along the column, which is due to the fact that the charges predominantly move forward and backward in the Coulomb well provided by their counterion.

In the system with a gate electrode the mobility per charge carrier decreases as the carrier density becomes larger. This can generate a new type of noise, which is caused by carrier numbers fluctuating on individual wires (cross talk between wires). The interaction noise can, in principle, be distinguished from other sources of noise. Also the frequency dependence of the charge carrier mobility is stronger when there are more charges on the column. In the stochastic limit, carrier–carrier interactions appear to produce random obstacles to the carrier motion, very much as if one introduced disorder into the system.

Finally, it should be noted that in this paper, we have not considered spin explicitly. We are working in a limit where Coulomb interactions prevent particles from crossing each other’s paths.

## ACKNOWLEDGMENTS

B.M. would like to thank the Leverhulme trust for a fellowship. The British Council and the Netherlands Organization for Scientific Research (NWO) are acknowledged for travel grants.

<sup>1</sup>N. Boden, R. J. Bushby, J. Clements, M. Jesudason, P. Knowles, and G. Williams, *Chem. Phys. Lett.* **152**, 94 (1988).

<sup>2</sup>S. Chandrasekhar and G. S. Raganath, *Rep. Prog. Phys.* **53**, 57 (1990).

<sup>3</sup>D. Adam, F. Closs, T. Frey, D. Funhoff, D. Haarer, H. Ringsdorf, P. Schumacher, and S. K. Siemensmeyer, *Phys. Rev. Lett.* **70**, 457 (1993).

<sup>4</sup>D. Adam, P. Schumacher, J. Simmerer, K. H. Eitzbach, H. Ringsdorf, and D. Haarer, *Nature (London)* **371**, 141 (1994).

<sup>5</sup>J. Clements, R. J. Bushby, B. Movaghar, N. Boden, K. Donovan, and T. Kreouzis, *Phys. Rev. B* **52**, 13274 (1995).

<sup>6</sup>J. Clements, R. J. Bushby, B. Movaghar, N. Boden, K. Donovan, and T. Kreouzis, *Phys. Rev. B* **33**, 3207 (1998).

<sup>7</sup>A. M. van de Craats, L. D. A. Siebbeles, I. Bleyl, D. D. Haarer, Y. A. Berlin, A. A. Zharikoy, and J. M. Warman, *J. Phys. Chem. B* **102**, 9625 (1998).

- <sup>8</sup>A. M. van de Craats and J. M. Warman, *J. Jap. Liq. Cryst. Soc.* **2**, 12 (1998).
- <sup>9</sup>A. M. van de Craats, J. M. Warman, A. Fechtenkötter, J. D. Brand, M. A. Harbinson, and K. Müllen, *Adv. Mater.* **11**, 1469 (1999).
- <sup>10</sup>J. M. Warman, M. P. de Haas, K. J. Smit, M. N. Paddon-Row, and J. F. van der Pol, *Mol. Cryst. Liq. Cryst.* **183**, 375 (1990).
- <sup>11</sup>D. Markovitsi, I. Lécuyer, P. Lianos, and J. Malthête, *J. Chem. Soc., Faraday Trans.* **87**, 1785 (1991).
- <sup>12</sup>T. Christ, V. Stümpflen, and J. H. Wendorff, *Macromol. Rapid Commun.* **18**, 93 (1997).
- <sup>13</sup>J. M. Warman and P. G. Schouten, *J. Phys. Chem.* **99**, 17181 (1995).
- <sup>14</sup>J. M. Warman, P. G. Schouten, G. H. Gelinck, and M. P. de Haas, *Chem. Phys.* **212**, 183 (1996).
- <sup>15</sup>P. G. Schouten, J. M. Warman, G. H. Gelinck, and M. J. Copyn, *J. Phys. Chem.* **99**, 11780 (1995).
- <sup>16</sup>N. Boden, R. J. Bushby, J. Clements, and B. Movaghar, *J. Appl. Phys.* **58**, 3063 (1998).
- <sup>17</sup>R. Y. Dong, D. Goldfarb, M. E. Moseley, and Z. Luz, *J. Phys. Chem.* **88**, 3148 (1984).
- <sup>18</sup>L. D. A. Siebbeles and B. Movaghar, *J. Chem. Phys.* **110**, 10162 (1999).
- <sup>19</sup>B. Movaghar, D. W. Murray, K. J. Donovan, and E. G. Wilson, *J. Phys. C* **17**, 1247 (1984).
- <sup>20</sup>U. Seiferheld, H. Baessler, and B. Movaghar, *Phys. Rev. Lett.* **51**, 813 (1983).
- <sup>21</sup>R. J. O. M. Hoofman, L. D. A. Siebbeles, M. P. d. Haas, A. Hummel, and D. Bloor, *J. Chem. Phys.* **109**, 1885 (1998).
- <sup>22</sup>R. J. O. M. Hoofman, L. D. A. Siebbeles, M. P. d. Haas, M. Szablewski, and D. Bloor, *Synth. Met.* **102**, 1417 (1999).
- <sup>23</sup>M. Rother, W. Wegscheider, F. Ertl, R. Deutschmann, M. Bichler, and G. Abstreiter, *Proceedings of the Namitech Workshop*, Stuttgart, 1999.
- <sup>24</sup>W. Wegscheider, M. Rother, G. Schedelbeck, M. Bichler, and G. Abstreiter, *Microelectron. Eng.* **47**, 215 (1999).
- <sup>25</sup>Z. Yao, H. W. C. Postma, L. Balents, and C. Dekker, *Nature (London)* **402**, 273 (1999).
- <sup>26</sup>N. Boden, R. J. Bushby, and J. Clements, *J. Chem. Phys.* **98**, 5920 (1993).
- <sup>27</sup>A. Bacher, I. Bleyl, C. H. Erdelen, D. Haarer, W. Paulus, and H. W. Schmidt, *Adv. Mater.* **9**, 1031 (1997).
- <sup>28</sup>H. Boettger and V. V. Bryskin, *Hopping Conduction in Solids* (Academie-Verlag, Berlin, 1985).
- <sup>29</sup>O. Hilt and L. D. A. Siebbeles, *Chem. Phys. Lett.* **269**, 257 (1997).
- <sup>30</sup>O. Hilt and L. D. A. Siebbeles, *Chem. Phys.* **229**, 257 (1998).
- <sup>31</sup>W. H. Press, B. P. Flannery, S. A. Teukolsky, and W. T. Vetterling, *Numerical Recipes* (Cambridge U.P., Cambridge, 1987).
- <sup>32</sup>G. Wegner, *Ber. Bunsenges. Phys. Chem.* **95**, 1326 (1991).
- <sup>33</sup>J. Clements, N. Boden, T. Gibson, R. Chandler, J. Hulbert, and E. A. Ruck-Keene, *Sens. Actuators B* **47**, 37 (1998).